



Contents lists available at ScienceDirect

NeuroImage: Clinical

journal homepage: [www.elsevier.com/locate/ynicl](http://www.elsevier.com/locate/ynicl)

# Thalamic functional connectivity predicts seizure laterality in individual TLE patients: Application of a biomarker development strategy

Daniel S. Barron<sup>a,b,\*</sup>, Peter T. Fox<sup>a,c,d,e,f</sup>, Heath Pardoe<sup>g</sup>, Jack Lancaster<sup>a,c</sup>, Larry R. Price<sup>h,i</sup>, Karen Blackmon<sup>g</sup>, Kristen Berry<sup>g</sup>, Jose E. Cavazos<sup>e,j</sup>, Ruben Kuzniecky<sup>g</sup>, Orrin Devinsky<sup>g</sup>, Thomas Thesen<sup>g</sup>

<sup>a</sup>Research Imaging Institute, University of Texas Health Science Center at San Antonio, San Antonio, TX, USA

<sup>b</sup>Yale University School of Medicine, New Haven, CT, USA

<sup>c</sup>Department of Radiology, University of Texas Health Science Center at San Antonio, San Antonio, TX, USA

<sup>d</sup>South Texas Veterans Health Care System, San Antonio, TX, USA

<sup>e</sup>Department of Neurology, University of TX Health Science Center, San Antonio, TX, USA

<sup>f</sup>State Key Lab for Brain and Cognitive Sciences, University of Hong Kong, Hong Kong

<sup>g</sup>Department of Neurology, New York University, New York, NY, USA

<sup>h</sup>College of Education, Texas State University, San Marcos, TX, USA

<sup>i</sup>College of Science, Texas State University, San Marcos, TX, USA

<sup>j</sup>San Antonio Epilepsy Center of Excellence, South Texas Veterans Health Care System, San Antonio, TX, USA

## ARTICLE INFO

### Article history:

Received 16 May 2014

Received in revised form 13 July 2014

Accepted 4 August 2014

Available online xxx

## ABSTRACT

Noninvasive markers of brain function could yield biomarkers in many neurological disorders. Disease models constrained by coordinate-based meta-analysis are likely to increase this yield. Here, we evaluate a thalamic model of temporal lobe epilepsy that we proposed in a coordinate-based meta-analysis and extended in a diffusion tractography study of an independent patient population. Specifically, we evaluated whether thalamic functional connectivity (resting-state fMRI-BOLD) with temporal lobe areas can predict seizure onset laterality, as established with intracranial EEG. Twenty-four lesional and non-lesional temporal lobe epilepsy patients were studied.

No significant differences in functional connection strength in patient and control groups were observed with Mann-Whitney Tests (corrected for multiple comparisons). Notwithstanding the lack of group differences, individual patient difference scores (from control mean connection strength) successfully predicted seizure onset zone as shown in ROC curves: discriminant analysis (two-dimensional) predicted seizure onset zone with 85% sensitivity and 91% specificity; logistic regression (four-dimensional) achieved 86% sensitivity and 100% specificity. The strongest markers in both analyses were left thalamo-hippocampal and right thalamo-entorhinal cortex functional connection strength. Thus, this study shows that thalamic functional connections are sensitive and specific markers of seizure onset laterality in individual temporal lobe epilepsy patients. This study also advances an overall strategy for the programmatic development of neuroimaging biomarkers in clinical and genetic populations: a disease model informed by coordinate-based meta-analysis was used to anatomically constrain individual patient analyses.

© 2014 Published by Elsevier Inc. This is an open access article under the CC BY-NC-ND license (<http://creativecommons.org/licenses/by-nc-nd/3.0/>).

## 1. Introduction

Temporal lobe epilepsy (TLE) is associated with brain pathology in gray and white matter network regions connected to the epileptogenic hippocampus (Spencer, 2002). Where brain pathology most commonly occurs and whether it could be used as a disease marker are of long-standing interest (Bouchet and Cazauviel, 1825; Margerison and

Corsellis, 1966; Keller and Roberts, 2008). The use of neuroimaging-based statistical biomarkers can guide the clinical evaluation of patients, particularly in complex cases without detectable lesions.

In our coordinate-based meta-analysis of medial TLE patients, we reported that the thalamus was the most common site of extra-hippocampal gray matter loss across 22 structural MRI experiments (Barron et al., 2012). This cross-study consensus informed our subsequent diffusion MRI study that reported decreased thalamo-hippocampal structural connectivity in an independent patient group (Barron et al., 2014). The present report further investigates this thalamo-hippocampal TLE model in another independent patient population using resting-state functional connectivity based on BOLD-fMRI.

\* Corresponding author. at: Office of Student Affairs, 367 Cedar St, New Haven, CT 06510, USA.

E-mail address: [daniel.s.barron@yale.edu](mailto:daniel.s.barron@yale.edu) (D.S. Barron).

Resting-state fMRI studies of TLE patients have reported functional connectivity changes in brain-wide analyses and anatomically constrained network models (Cataldi, Avoli and de Villiers-Sidani, 2013). Such changes could inform further clinical assessment of TLE patients in terms of where to place intracranial EEG grids, particularly those without detectable lesions on structural MRIs. Previous reports have used functional connection strength to lateralize seizure onset: Bettus et al. (2010) reported an anatomically constrained network analysis within the medial temporal lobe and Morgan et al. (2012) reported a brain-wide (voxel-wise) analysis with the hippocampus (see Discussion for details). Per our previously reported TLE model, our study presents a novel, anatomically constrained network analysis of thalamic connectivity with the hippocampus, amygdala, and entorhinal cortex. To the best of our knowledge, no previous studies have evaluated an anatomically constrained model of thalamic functional connectivity.

The present study investigates the effect of TLE laterality on thalamic resting-state functional connectivity and whether thalamic connectivity has predictive value as a marker of seizure onset laterality. We compare functional connectivity strength between the thalamus, hippocampus, amygdala, and entorhinal cortex to predict whether individual patients have right or left seizure onset in separate discriminant and logistic regression analyses. Prediction efficacy is evaluated with standard performance measures and receiver operating characteristic (ROC) curves.

## 2. Methods

### 2.1. Subjects

Twenty-four right handed TLE patients (11 males, 13 females) and 20 age-matched controls were enrolled in the study from 2006 to 2013, see Table 1 for demographic information. All participants consented to the study's protocol approved by New York University's Institutional Review Board, and represent separate populations from previous work

(Barron et al., 2012; Barron et al., 2014). Participants were referred for structural and functional MRI by clinicians at NYU's Comprehensive Epilepsy Center. Twenty of the 24 TLE patients were candidates for surgical resection of epileptogenic tissue, and received iEEG monitoring to confirm diagnosis and rule out additional epileptogenic areas prior to resective surgery. See Table 2 for clinical information. Each patient received a seizure onset lateralization code that was used as the "gold-standard." This lateralization code was established by iEEG when available and video EEG when unavailable. Lesions were identified through visual inspection of structural MRI by a radiologist. In addition, individual left and right hippocampal volumes were tested for significantly reduced volumes compared to a control population (see eMethods). Localization of seizure onset was determined by iEEG or video EEG. Lateralization codes based on electrophysiological recordings matched the lateralization of unilateral lesions and/or statistical hippocampal volume differences when present.

### 2.2. Image acquisition

Each subject underwent a single MRI session with a 3.0 T Siemens Allegra scanner. Sequences included a whole brain T1 weighted MPRAGE sequence optimized for gray-white contrast (TR/TE = 2530/3.25 ms; FA = 8°; matrix size = 256 × 256 × 128; FOV = 256 mm; voxel size = 1 × 1 × 1.3 mm<sup>3</sup>) and a resting-state fMRI-BOLD multi-slice gradient-recalled echo planar imaging acquisition (TR = 2 s, FOV = 192 mm; 197 volumes, voxel size 3 × 3 × 3 mm<sup>3</sup>) while patients lay in the scanner with their eyes open.

### 2.3. VOI definition

Volumes of interest (VOI) for the thalamus, hippocampus, amygdala, and entorhinal cortex were created using the Freesurfer (5.1; <http://surfer.nmr.mgh.harvard.edu>) recon-all function. In this procedure image volumes are resampled from native T1 image space to 1 mm isotropic space; segmentations are generated in 1 mm space then mapped

**Table 1**  
Demographic information.

Patient	Sex	Handed <sup>a</sup>	Age sz onset	Sz freq. <sup>b</sup>	Wada language	Wada L memory	Wada R memory	GCF <sup>c</sup>	VCI <sup>d</sup>	POI <sup>e</sup>	WMI <sup>f</sup>	PSI <sup>g</sup>
1	F	R	17	1/m	L	10	10	Borderline impaired	77	67	—	—
2	F	R	6	2–3/m	L	5	11	Low avg	96	74	93	91
3	F	R	6	3–4/d	L	3	5	Low avg	82	103	88	93
4	F	R	32	1–2/d	—	—	—	Avg	98	96	100	102
5	F	R	—	—	L	4	11	Avg	102	105	108	94
6	M	R	—	1–4/m	L	10	12	Avg	107	102	105	108
7	F	R	5	2/y	B	4	10	Low avg	76	80	85	73
8	M	R	35	6 total	B	12	8	Avg	107	99	108	91
9	F	R	23	1/w	B	10	12	Superior	110	133	111	93
10	F	R	29	1–2/m	L	12	11	High avg	118	123	127	108
11	M	R	5	3.5/m	R	1	10	Borderline impaired	—	—	—	—
12	F	R	31	2/m	L	2	5	—	—	—	—	—
13	F	R	1	1/m	L	9	2	Avg	—	95	—	81
14	M	R	10	1–4/w	L	5	4	Superior	150	111	131	122
15	M	R	'Child'	2–3/d	L	12	0	—	—	—	—	—
16	F	R	—	3/m	L	11	5	Impaired	72	69	69	62
17	M	R	17	1/d	B	12	12	Avg	96	104	86	100
18	M	R	21	1/m	L	11	11	Low avg	75	—	86	75
19	F	R	7	0–2/m	L	11	9	Avg	109	116	91	108
20	F	R	28	3–4/w	—	—	—	Avg	125	88	114	89
21	M	R	29	2–3/w	L	12	8	Above avg	125	105	128	111
22	M	R	—	10–15/m	L	12	0	Superior	125	128	—	—
23	M	R	—	—	L	10	6	Avg	—	—	—	—
24	M	R	14 m	—	—	—	—	Impaired	76	50	55	76

<sup>a</sup> R = right.

<sup>b</sup> Self-reported, m = month, w = week, d = day.

<sup>c</sup> General cognitive function.

<sup>d</sup> Verbal comprehension index.

<sup>e</sup> Personal orientation inventory.

<sup>f</sup> Working memory inventory.

<sup>g</sup> Psychological screening.

t2.1 **Table 2**  
t2.2 Classification of laterality and corresponding clinical information.

t2.3	Patient	Laterality classification <sup>a</sup>	HS <sup>b</sup>	Lesion <sup>c</sup>	iEEG?	Sz onset <sup>d</sup>	Resection location	Engel outcome
t2.4	1	Left	L	L MTS	Y	L MT	L AT, HPC	Engel 1
t2.5	2	Left	L	L MTS	N	L T (vEEG)	N/A	N/A
t2.6	3	Left	L	L MTS	Y	L MT	L AT, HPC	Engel 4
t2.7	4	Left	L	L MTS	N	L T (vEEG)	N/A	N/A
t2.8	5	Left	L	L HPC infarct	Y	L MT	L AT, HPC	Engel 1
t2.9	6	Left	L	No	Y	L MT & middle TL	L Inferior AT	Engel 1
t2.10	7	Left	B	No	Y	L MT	L AT, HPC	Engel 1
t2.11	8	Left		No	Y	L MT	L AT, HPC	Engel 2
t2.12	9	Left		No	Y	L MT	L AT, HPC	Engel 1
t2.13	10	Left		L HPC & BT dysgenesis	N	L T & F (vEEG)	N/A	N/A
t2.14	11	Left		L MTS	Y	L MT	L AT, HPC, AMY	Engel 1
t2.15	12	Left		L T cyst	Y	L MT	L AT, HPC	Engel 1
t2.16	13	Right	R	No	Y	R MT	R AT	Engel 1
t2.17	14	Right	R	T gliosis	Y	R MT & R O	R AT & R O	Engel 1
t2.18	15	Right	R	R MTS	Y	R MT	R AT, HPC, AMY	Engel 3
t2.19	16	Right	R	R MTS	Y	R MT & mid T	R AT, HPC, AMY	Engel 2
t2.20	17	Right	R	R MTS	Y	R MT	R AT, HPC, AMY	Engel 1
t2.21	18	Right	B	CC & parietal hypoplasia	Y	R MT	R AT, HPC	Engel 1
t2.22	19	Right		R Parietal-occipital cystic lesion	Y	R MT, R mesial O	R AT, R mesial O, & HPC	Engel 1
t2.23	20	Right		R MTS	N	RT & F (vEEG)	N/A	N/A
t2.24	21	Right		R PT cavernoma	Y	R MT & PT	R AT & PT cavernoma	Engel 2
t2.25	22	Right		R MTS	Y	R MT, AT, & mid T	R AT, HPC	Engel 1
t2.26	23	Right		No	Y	R MT	R AT, HPC, AMY	Engel 3
t2.27	24	Right		No	Y	R TL & MF	No resection	N/A

t2.28 Abbreviations: MTS = medial temporal sclerosis, T = temporal, O = occipital, F = frontal, AT = anterior temporal, PT = posterior temporal, M = mesial, HPC = hippocampus, AMY =  
t2.29 amygdala, BT = basal temporal, CC = corpus callosum.

t2.30 <sup>a</sup> Classification of laterality established by iEEG and vEEG and used in connectivity analysis.

t2.31 <sup>b</sup> Significantly lower hippocampal volumes compared to control population.

t2.32 <sup>c</sup> Lesions identified by radiologist's visual inspection of MRI.

t2.33 <sup>d</sup> Localization of seizure onset established by iEEG or when unavailable, vEEG as indicated.

125 back onto native image space. These tools have been validated by refer- 156  
126 ence to manual thalamus (Keller et al., 2012) and hippocampus (Pardoe 157  
127 et al., 2009) labeling in healthy subjects and epilepsy patients. Anterior 158  
128 and posterior hippocampal VOIs were created in individual patients by 159  
129 dividing the hippocampal VOI (described above) by a coronal plane at 160  
130 its anterior–posterior center. These anterior and posterior divisions 161  
131 were created to, in part, replicate the Bettus et al. (2010) study (Fig. 1). 162

#### 132 2.4. Resting-state fMRI pre-processing

133 Resting-state fMRI image volumes were pre-processed according to 158  
134 the Weissenbacher et al. (2009) procedure by applying FSL tools within 159  
135 the MatLab environment. Further information may be referenced in 160  
136 eMethods. 161

#### 137 2.5. Correlation, Mann–Whitney test, and effect size analysis

138 Mean time series signals were extracted from individual VOIs 158  
139 (fslmeants, implemented in MatLab) to produce 6 time series per hemi- 159  
140 sphere per subject (thalamus, hippocampus, amygdala, entorhinal 160  
141 cortex, anterior hippocampus, and posterior hippocampus). For each 161  
142 patient,  $p$ , and healthy control,  $hc$ , the Pearson product mean correlation 162  
143 coefficient was calculated resulting in a  $12 \times 12$  cross correlation matrix, 163  
144 which was transformed to produce a Fischer z-score cross correlation 164  
145 matrix,  $FC$ , for each subject. These  $FC$  matrices represent a standardized 165  
146 parameter of functional connectivity and were used to investigate 166  
147 group differences using Mann–Whitney (Glantz, 2012) and effect size 167  
148 (Cohen et al., 1996) tests. Details about these tests may be referenced 168  
149 in eMethods. 169

150 Individual patient difference scores were calculated as individual 170  
151 patients' Fisher z-score matrix minus the control group mean Fischer 171  
152 z-score matrix ( $FC_p - \bar{FC}_{hc} = Q_p$ ). For each patient, this yielded a 172  
153  $12 \times 12$  difference score matrix,  $Q_p$ , illustrating the difference in 173  
154 connection strength for connection  $Z_1, Z_2, \dots, Z_j, \dots, Z_{66}$  in a patient  $p$  174  
155 compared to the baseline control. Difference scores were used to 175

determine seizure onset laterality in separate discriminant and log- 156  
515 stic regression analyses. 157

Data were further analyzed using discriminant and logistic regression 158  
516 analyses. Discriminant analysis performs group classification based on a 159  
517 continuous independent variable. Here, discriminant analysis classified 160  
518 patients as either “L” or “R” seizure onset group based on 2 difference 161  
519 scores of functional connectivity strength. Logistic regression is an alter- 162  
520 native to group classification wherein the likelihood of group member- 163  
521 ship is expressed as a probability. Here, logistic regression computed 164  
522 the probability that a particular patient had right seizure onset (the alter- 165  
523 native being left seizure onset) based on up to 6 difference scores. Fur- 166  
524 ther details about these analyses, including criteria used to select the 167  
525 difference scores used therein, may be referenced in eMethods. The accu- 168  
526 racy of discriminant analysis and logistic regression was computed with 169  
527 standard performance measures (sensitivity, specificity, positive predic- 170  
528 tive value, and negative predictive value) and with an ROC curve (cf. 171  
529 Table 3 and Fig. 3). 172

### 173 3. Results

#### 174 3.1. Group comparison: Mann–Whitney tests

Group differences in functional connection strength were evaluated 175  
530 with Mann–Whitney tests (Glantz, 2012). Significant group differences 176  
531 ( $p < 0.05$ , FDR correction for multiple comparisons) in functional con- 177  
532 nectivity were only observed for physiological identities, or correlations 178  
533 between the hippocampi and their ipsilateral (composite) anterior/ 179  
534 posterior divisions. No other significant group differences were ob- 180  
535 served. There was a trend for R-TLE to have increased functional connec- 181  
536 tivity within left hemispheric regions while L-TLE showed decreased 182  
537 connectivity within left hemispheric regions. In addition, there was a 183  
538 general trend for the L-TLE group to have increased functional connectiv- 184  
539 ity between the left thalamus and left hippocampus, between the right 185  
540 thalamus and left thalamus, and between the right hippocampus and 186  
541 left hippocampus. These trends are plotted in color as cross-correlation 187  
542 matrices in eFigure 1. 188

**Table 3**  
Summary of discriminant and logistic regression analyses.

Patient number	HS <sup>a</sup>	Actual group 0 = L; 1 = R	Discriminant analysis (2 predictors <sup>b</sup> )								Logistic regression (4 predictors <sup>c</sup> )				
			No bootstrap				Bootstrap (n = 1000)				No bootstrap		Bootstrap (n = 1000)		
			Original		Cross-validation		Original		Cross-validation		Group	P (p = 1)	Group	P (p = 1)	
			Group	P (p = 1)	Group	P (p = 1)	Group	P (p = 1)	Group	P (p = 1)	Group	P (p = 1)	Group	P (p = 1)	
t3.4	1	L	0	0	0.10	0	0.11	0	0.10	0	0.11	0	.094	0	.094
t3.5	2	L	0	0	0.44	0	0.49	0	0.44	0	0.49	0	.115	0	.115
t3.6	3	L	0	0	0.09	0	0.10	0	0.09	0	0.10	0	.267	0	.267
t3.7	4	L	0	0	0.00	0	0.00	0	0.00	0	0.00	0	.000	0	.000
t3.8	5	L	0	0	0.11	0	0.12	0	0.11	0	0.12	0	.216	0	.216
t3.9	6	L	0	0	0.03	0	0.04	0	0.03	0	0.04	0	.009	0	.009
t3.10	7	B	0	0	0.06	0	0.07	0	0.06	0	0.07	0	.080	0	.080
t3.11	8		0	1**	0.62	1**	0.67	1**	0.62	1**	0.67	0	.475	0	.475
t3.12	9		0	0	0.02	0	0.02	0	0.02	0	0.02	0	.029	0	.029
t3.13	10		0	0	0.03	0	0.04	0	0.03	0	0.04	0	.016	0	.016
t3.14	11		0	0	0.31	0	0.33	0	0.31	0	0.33	0	.378	0	.378
t3.15	12		0	0	0.04	0	0.04	0	0.04	0	0.04	0	.035	0	.035
t3.16	13	R	1	1	0.66	0**	0.17	1	0.66	0**	0.17	1	.975	1	.975
t3.17	14	R	1	1	0.90	1	0.89	1	0.90	1	0.89	1	.996	1	.996
t3.18	15	R	1	1	0.66	1	0.64	1	0.66	1	0.64	1	.898	1	.898
t3.19	16	R	1	1	0.94	1	0.93	1	0.94	1	0.93	1	.982	1	.982
t3.20	17	R	1	1	1.00	1	1.00	1	1.00	1	1.00	1	.999	1	.999
t3.21	18	B	1	0**	0.17	0**	0.08	0**	0.17	0**	0.08	0**	.091	0**	.091
t3.22	19		1	0**	0.21	0**	0.13	0**	0.21	0**	0.13	0**	.394	0**	.394
t3.23	20		1	1	0.96	1	0.96	1	0.96	1	0.96	1	.984	1	.984
t3.24	21		1	1	0.95	1	0.94	1	0.95	1	0.94	1	.968	1	.968
t3.25	22		1	1	0.99	1	0.99	1	0.99	1	0.99	1	1.000	1	1.000
t3.26	23		1	1	0.97	1	0.97	1	0.97	1	0.97	1	.998	1	.998
t3.27	24		1	1	1.00	1	1.00	1	1.00	1	1.00	1	1.000	1	1.000
t3.28															
			Discriminant analysis (2 predictors <sup>b</sup> )								Logistic regression (4 predictors <sup>c</sup> )				
			No bootstrap				Bootstrap (n = 1000)				No bootstrap		Bootstrap (n = 1000)		
			Original		Cross-validation		Original		Cross-validation						
t3.29			Sensitivity	85%	79%	85%	79%	86%	86%						
t3.30			Specificity	91%	90%	91%	90%	100%	100%						
t3.31			PPV <sup>d</sup>	92%	92%	92%	92%	100%	100%						
t3.32			NPV <sup>d</sup>	83%	75%	83%	75%	83%	83%						

t3.33 <sup>a</sup> Hippocampal sclerosis determined by volumetric analysis, see eMethods, L = left, R = right, B = bilateral.  
t3.34 <sup>b</sup> 2 predictors = individual differences in connectivity between left thalamus and left hippocampus and between right thalamus and right entorhinal cortex.  
t3.35 <sup>c</sup> 4 predictors = individual differences in connectivity between left thalamus and left hippocampus, between right thalamus and right entorhinal cortex, between left amygdala and left  
t3.36 amygdala, and between right posterior hippocampus and left anterior hippocampus.  
t3.37 <sup>d</sup> PPV = positive predictive value, NPV = negative predictive value, both PPV and NPV were calculated based on our sample population.

189 3.2. Group effects: effect size analysis

190 The group effect of seizure onset laterality was evaluated with stan-  
191 dard effect size tests (Cohen et al., 1996). Medium effect sizes (>.3 as  
192 Q7 defined by Cohen (1988)) were observed for connections between the  
193 left thalamus and left hippocampus (0.43), left amygdala (0.46), and  
194 left anterior hippocampus (0.46); between the right posterior hippo-  
195 campus and left hippocampus (−0.33) and left posterior hippocampus  
196 (−0.33); between the right thalamus and left amygdala (0.34); and be-  
197 tween the right entorhinal cortex and right thalamus (−0.30) (See  
198 Fig. 2 and eTable 2).

199 Six connections met our criteria for suitable predictors of seizure  
200 onset laterality. These connections are described below in reference to  
201 their usage in the discriminant and logistic regression analyses. The se-  
202 lection criteria for these connections are explained in eMethods and are  
203 Q8 presented in tabular form in eTable 3.

204 3.3. Group classification: discriminant analysis

205 A direct discriminant analysis was performed using 2 functional con-  
206 nection strengths to determine group classification. The 2 functional  
207 connections were between the left thalamus and left hippocampus  
208 (modeled as “predictor 1”) and between the right entorhinal cortex  
209 and the right thalamus (modeled as “predictor 2”). Individual patients  
210 were classified into right (modeled as “1”) and left (modeled as “0”) sei-  
211 zure onset groups. One discriminant function was generated ( $\lambda = .42$ ;

$\chi^2 (2, N = 24) = 18.2$ ;  $p < .001$ ) and indicated that the function of the 212  
213 predictors significantly differentiated between patients’ laterality. Group  
214 classification (laterality) explained 100% of function variance. Predictor  
215 1 was most associated with the function (e.g., 1.123 – standardized func-  
216 tion. 57 – correlation with discriminant function).

217 Discriminant analysis predicted seizure onset laterality with a sensi-  
218 tivity of 85% and a specificity of 91% (cross-validation of the discrimi-  
219 nant analysis was similar: 79% sensitivity, 90% specificity). For the  
220 sample, 87.5% of the original cases were correctly classified and 83% of  
221 the cases were correctly classified in the cross-validation analysis, de-  
222 scribed in eMethods. An ROC curve showed that the discriminant anal-  
223 ysis of original cases was significantly different from a completely  
224 random group assignment ( $p < .0001$ ). Cross-validation analysis was  
225 also significant ( $p < .001$ ). Individual patient results, additional perfor-  
226 mance measures, discriminant analysis parameter estimates, and stan-  
227 dard errors for the bootstrap analysis are reported in Table 3. See  
228 Fig. 3 for full ROC parameters.

229 3.4. Group probability: logistic regression analysis

230 Six logistic regression analyses were performed using 1 through 6  
231 functional connection strengths to predict the probability of seizure  
232 onset laterality. The logistic regression with four predictors yielded  
233 the most reliable parameter estimates, with the standard error for  
234 each predictor being less than 4.2. These four predictors represented  
235 connectivity strength between the: left thalamus and left hippocampus,



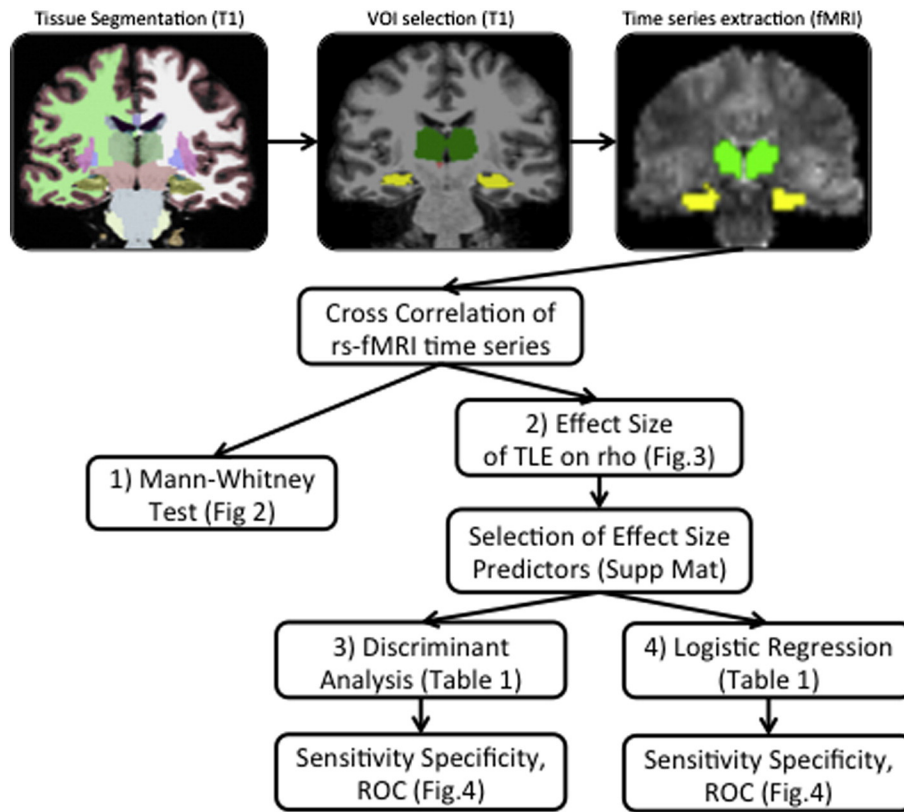


**Fig. 1.** Analysis overview. Individual subject structural MRI image volumes were segmented and the thalamus, hippocampus, amygdala, and entorhinal cortex volumes of interest (VOIs) were transformed to functional MRI space. Within these VOIs, mean time series were extracted and cross correlations were computed. 1) Group comparisons were performed with Mann-Whitney tests. 2) The effect size of individual patient's TLE on rho was compared to corresponding mean of healthy controls (n = 20). 3) Discriminant analysis and 4) logistic regression were performed to predict seizure onset laterality from functional connectivity effect size. Selection of effect size predictors is described in eMethods and supplementary materials.

236 modeled as “predictor 1”; right thalamus and right entorhinal cortex,  
 237 “predictor 2”; right amygdala and left hippocampus, “predictor 3”; and  
 238 right posterior hippocampus and left anterior hippocampus, “predictor  
 239 4”. Based on the Wald criterion at the four predictor logistic regression,  
 240 only “predictor 2” was significant (p = 0.05). Lack of significance was  
 241 due to large standard errors of estimated beta weights as a byproduct  
 242 of performance of the maximum likelihood estimator under small sam-  
 243 ple size (Keller et al., 2014; Hosmer et al., 2013). See eTable 4 for a

244 summary of difference scores utilized and parameters from all six logistic  
 245 regressions including regression coefficients, Wald statistics, odds ratios,  
 246 and 95% confidence intervals for odds ratios.

247 A test of the full model with four predictors against a constant-only  
 248 model was statistically significant,  $\chi^2$  (df = 4, N = 24) = 22.064,  
 249 p < .001, indicating that as a set, the predictors reliably distinguished be-  
 250 tween R and L TLE patients. The variance accounted for in classification  
 251 was large, Nagelkerke R = .802. These four connections predicted

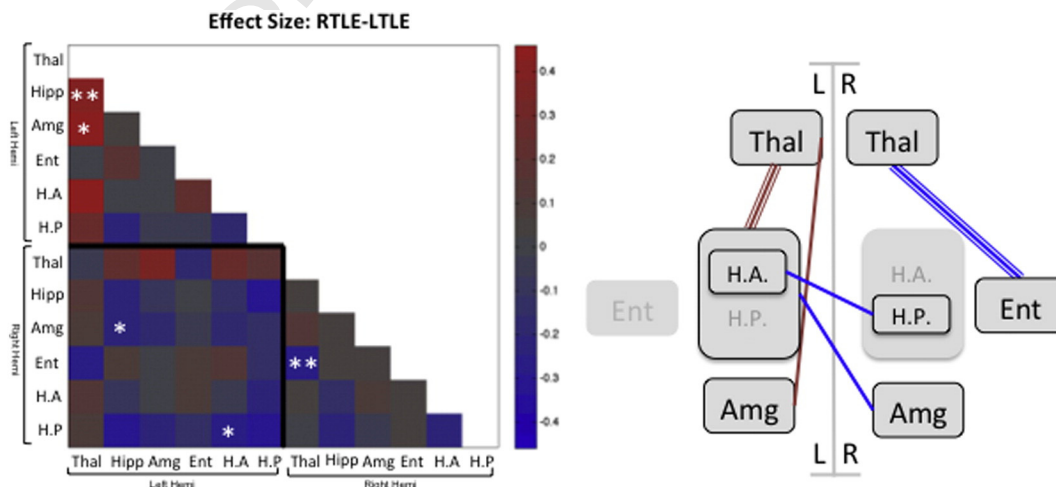


**Fig. 2.** Effect size of TLE laterality on functional connectivity. Left: effect size was calculated as the difference of group averaged Fischer transformed correlation coefficients for R (red) and L (blue) TLE patients subtracted from the control group mean (Cohen, 1988). Effect sizes used as predictors for discriminant analysis are denoted with \* and those used for logistic regression denoted with both \* and \*\*. To improve clarity of the figure, the redundant upper triangle of the matrix has been excluded. Right: diagram of effect sizes used to predict seizure onset laterality. Red lines represent increased functional connectivity compared to control; blue lines represent decreased. Triple lines represent effect sizes used in discriminant analysis; logistic regression used both triple and single lines.

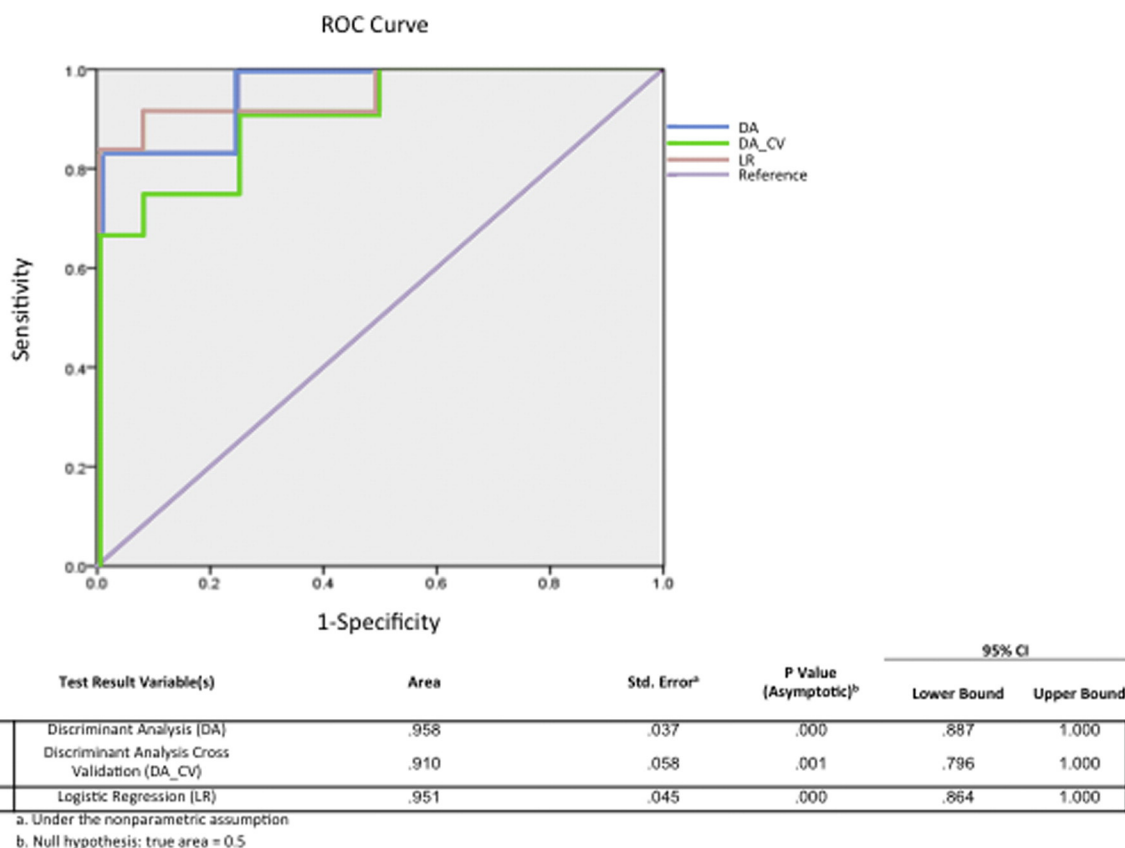


**Fig. 3.** ROC curve of discriminant and logistic regression analysis methods. Curve is based on individual patient data reported in Table 3. Discriminant analysis probabilities were adjusted to be relative to diagnosis of RTLE,  $P(p = 1)$ .

laterality with a sensitivity of 86% and a specificity of 100% (other performance characteristics, see Table 3 & Fig. 3). Notwithstanding the small sample size, analyses with and without bootstrapping achieved identical results. Individual patient laterality predictions can be referenced in Table 3.

#### 4. Discussion

This study demonstrates that inter-regional resting-state functional connectivity predicts the hemisphere of seizure onset in individual TLE patients. Consistent with our previously proposed network model of TLE, the strongest predictors of seizure onset laterality were connectivity strength between the left thalamus and left hippocampus and between the right thalamus and right entorhinal cortex. Using these connection strengths, discriminant analysis and logistic regression predicted seizure onset laterality with high sensitivity and specificity.

##### 4.1. Anatomically constrained analyses outperform brain-wide analyses

Using a novel strategy and statistical method, we found that thalamic connectivity was the strongest predictor of seizure onset in patients with TLE. Our goal was to determine which network connections would be most affected by TLE laterality and therefore be most predictive of seizure onset laterality. Based on a previously proposed (Barron et al., 2012) and confirmed (Barron et al., 2014) thalamic model of TLE network damage, this study performed a functional connectivity analysis between the thalamus, hippocampus, amygdala, and entorhinal cortex.

Bettus et al. (2010) reported an anatomically constrained analysis that detected TLE-related changes in functional connections between the posterior hippocampus and amygdala and between the anterior hippocampus and posterior hippocampus. These connection strengths

lateralized seizure onset zone with 64% sensitivity and 91% specificity. For this reason, the amygdala, entorhinal cortex, and anterior and posterior hippocampal divisions were included as seeds in our analysis of thalamic connectivity.

Morgan et al. (2012) reported a brain-wide (voxel-wise) functional connectivity analysis between the whole hippocampus and each brain voxel. Altered connectivity between the right hippocampus and 5 thalamic voxels lateralized the seizure onset zone with 100% sensitivity and 87.5% specificity in 7 patients. We attempted to replicate this analysis in our 23 patient sample by analyzing hippocampal connectivity in two ways: first to each thalamic voxel (as in Morgan et al., 2012) and then to each thalamic nucleus (as defined in Krauth et al., 2010). In both analyses, individual patient difference scores varied greatly and were not consistently predictive of laterality. We observed that the smaller the volume analyzed, the more variable the measurement across subjects (data unreported). That is, the voxel-wise analysis performed less well than the per-nucleus analysis, which performed less well than the regional-thalamus analysis (reported here).

##### 4.2. Framework for thalamic involvement in TLE

Because thalamic connections were the most predictive of TLE laterality, we now propose a framework for thalamic involvement in TLE. Thalamic involvement in TLE seizure initiation (Spencer, 2002), propagation (Guye, 2006), and spread (Bertram et al., 2008) is supported by a large and growing literature. Thalamic atrophy is correlated to medial temporal lobe (MTL) atrophy in volumetric (Bernhardt et al., 2012), diffusion tractography (Keller et al., 2014), and T2 weighted studies (Keller et al., 2014). In comparison to neocortical atrophy, thalamic atrophy is relatively uncorrelated to disease duration (Coan et al., 2014). Together, these observations imply that thalamic involvement differs with disease progression and suggests stage-specific

involvement of thalamic nuclei. The thalamic medial dorsal nucleus is the most consistent site of gray matter reduction reported in structural MRI studies (Barron et al., 2012), suggesting that the medial dorsal nucleus represents an early “damaged” pathway in TLE. Notwithstanding decreased thalamic structural connectivity with the temporal lobe in medial TLE patients (Keller et al., 2014), the medial pulvinar remained the most structurally connected thalamic nucleus (Barron et al., 2014), suggesting that the medial pulvinar represents a consistently “open” pathway.

Given the observations of midline thalamic atrophy (Bernhardt et al., 2012), we propose that epileptogenic damage to the anterior and medial dorsal nuclei facilitates TLE seizure onset (per Coan et al., 2014), while damage to the medial pulvinar facilitates seizure generalization (Rosenberg et al., 2009). Such a framework provides further anatomical basis for the concept that network disruption (as opposed to a single, focal disruption) causes seizures (Cavazos and Cross, 2006). Neuroimaging supports this framework, however, definitive nucleus-specific electrophysiological studies are required as a formal validation.

#### 4.3. Interpretation of predictors

Thalamo-hippocampal functional connection strength was the strongest predictor of seizure onset laterality in both our discriminant analysis and logistic regression analysis. Thalamo-entorhinal cortex connection strength was the second strongest predictor. Both of these novel findings are consistent with known physiology, as follows.

Physiological synchronization between the thalamus and MTL structures has been described during TLE seizure (electrophysiology (Guye, 2006)) and at rest (fMRI (Cataldi et al., 2013)). The entorhinal cortex is the main excitatory input to the hippocampus and is known to significantly interact with the hippocampus at seizure onset (Guye, 2006; Bartolomei et al., 2005), likely via CA1 and subicular hippocampal connections, which reorganize during epileptogenesis (Cavazos and Cross, 2006; Witter, 1993). Ictal electrophysiological synchronization of the entorhinal cortex with the thalamus occurs before hippocampal synchronization with the thalamus, suggesting that whatever influence the thalamus exerts on the hippocampus acts via the entorhinal cortex (Guye, 2006).

For both predictors, no comparable effects in the opposite hemisphere were observed, i.e. left thalamo-hippocampal connectivity was increased in L compared to R-TLE patients but right thalamo-hippocampal connectivity was not increased in R compared to L-TLE patients. One explanation could be that R and L-TLE affect network connectivity in different ways, as demonstrated by Bernhardt et al. (2011) and Karunanayaka et al. (2011). Another explanation could be that left and right thalamo-hippocampal connections are differentially engaged during the resting state. The presence of lateralized attention (right hemisphere) and language (left hemisphere) networks during the resting state supports this idea. While neuropsychological measures of language ability are known correlates of L-TLE, the relation of R-TLE to attention set switching and maintenance is relatively unknown. Further investigation of these measures in relation to functional connectivity strength could therefore prove useful.

#### 4.4. Biomarker discovery

The strategy and results presented seek to identify a biomarker using an anatomically constrained model of TLE. It is notable that while multiple differences in connection strength were useful predictors of seizure onset laterality, no one connection significantly differed from controls in group-level comparisons. In terms of biomarker identification, our results argue that the absence of a significant group-level difference should not discourage efforts to assess the clinical utility of multiple differences at the individual-level. Such an approach may be optimized when investigating the predictive effects of a disease model informed by coordinate-based meta-analysis, as done here.

#### 4.5. Limitations

Functional connectivity is an operative term applied to temporally correlated, spatially remote neurophysiological events (Friston, 1994). As applied here, functional connectivity represents temporal correlations in the mean fMRI-BOLD time-series signal of particular tissue volumes acquired under the resting condition. While functional connectivity is not intended to imply structural connectivity, our results are consistent with previous reports investigating structural connectivity (Barron et al., 2014; Keller et al., 2014).

Although the patient sample studied ( $n = 24$ ) is relatively large for an fMRI study, a larger cohort would increase the rigor of these results. Because of concerns about small sample size, we performed discriminant analysis and logistic regression with and without bootstrapping ( $n = 1000$ ); identical results were achieved. We addressed concerns of model “over-fitting” in the discriminant analysis by inclusion of a leave-one-out cross-validation. This step yielded a small decrease in prediction performance, however served as a validation of the specific analytic model built and used in the discriminant analysis. While the overall strategy of building a disease model with coordinate-based meta-analysis may reasonably be tested in other neurological disorders, the specific disease model tested in the present analysis is specific to the TLE population. As such, the sensitivity and specificity metrics reported above are limited to the TLE population.

Notwithstanding these limitations, the present study further confirms our previously proposed TLE disease model in an independent patient population using different methods.

#### 5. Conclusion

Thalamic functional connectivity can predict seizure onset laterality in TLE patients with and without hippocampal sclerosis. This study advances an overall strategy for the programmatic development of neuroimaging biomarkers in clinical and genetic populations: a disease model informed by coordinate-based meta-analysis was used to anatomically constrain individual patient analyses.

#### Conflict of interests disclosure

None reported.

#### Funding/support

Funding from the National Institute of Neurological Disorder & Stroke 1-F31-NS083160-01 (D.S.B.), National Institute of Health RO1 MH074457 (P.T.F.), F.A.C.E.S (Finding a cure for epilepsy and Seizures; T.T., O.D.) and the American Epilepsy Foundation (T.T.) assisted in the collection, management, analysis, and interpretation of the data; and in the preparation and review of the manuscript.

#### Acknowledgments

The authors thank Kristin S. Budde (BA, MD, MPH, Yale University) for her review of the manuscript; Xiuyuan Wang (BS, MS, New York University) for his technical assistance with MatLab; and Callah Boomhaur (BA, New York University) for her administrative assistance. Daniel S. Barron had full access to all of the data in the study and takes responsibility for the integrity of the data and the accuracy of the data analysis.

#### Supplementary material

Supplementary material for this article can be found online at <http://dx.doi.org/10.1016/j.nicl.2014.08.002>.

423 **References**

- 424 Barron, D.S., Fox, P.M., Laird, A.R., Robinson, J.L., Fox, P.T., 2012. Thalamic medial dorsal nu-  
425 cleus atrophy in medial temporal lobe epilepsy: a VBM meta-analysis. *NeuroImage*.  
426 *Clinical 2*, 25–32. <http://dx.doi.org/10.1016/j.nicl.2012.11.00424179755>.
- 427 Barron, D.S., Tandon, N., Lancaster, J.L., Fox, P.T., 2014. Thalamic structural connectivity in  
428 medial temporal lobe epilepsy. *Epilepsia* 2014, e50–e55. <http://dx.doi.org/10.1111/epi.1263724802969>.
- 430 Bartolomei, F., Khalil, M., Wendling, F., et al., 2005. Entorhinal cortex involvement in human  
431 mesial temporal lobe epilepsy: an electrophysiologic and volumetric study. *Epilepsia* 46  
432 (5), 677–687. <http://dx.doi.org/10.1111/j.1528-1167.2005.43804.x15857433>.
- 433 Bernhardt, B.C., Chen, Z., He, Y., Evans, A.C., Bernasconi, N., 2011. Graph-theoretical analysis  
434 reveals disrupted small-world organization of cortical thickness correlation networks  
435 in temporal lobe epilepsy. *Cerebral Cortex* (New York, N.Y.: 1991) 21 (9), 2147–2157.  
436 <http://dx.doi.org/10.1093/cercor/bhq29121330467>.
- 437 Bernhardt, B.C., Bernasconi, N., Kim, H., Bernasconi, A., 2012. Mapping thalamocortical net-  
438 work pathology in temporal lobe epilepsy. *Neurology* 78 (2), 129–136. <http://dx.doi.org/10.1212/WNL.0b013e31823efd0d22205759>.
- 440 Bertram, E.H., Zhang, D., Williamson, J.M., 2008. Multiple roles of midline dorsal thalamic  
441 nuclei in induction and spread of limbic seizures. *Epilepsia* 49 (2), 256–268. <http://dx.doi.org/10.1111/j.1528-1167.2007.01408.x18028408>.
- 442 Bettus, G., Bartolomei, F., Confort-Gouny, S., et al., 2010. Role of resting state functional  
443 connectivity MRI in presurgical investigation of mesial temporal lobe epilepsy. *Journal of Neurology, Neurosurgery, and Psychiatry* 81 (10), 1147–1154. <http://dx.doi.org/10.1136/jnnp.2009.19146020547611>.
- 444 Bouchet, M.M., Cazauvieilh, J.B., 1825. De l'épilepsie considérée dans ses rapports avec  
445 l'aliénation mentale. *Archives générales de Médecine* 9, 510–542.
- 449 Cataldi, M., Avoli, M., de Villiers-Sidani, E., 2013. Resting state networks in temporal lobe  
450 epilepsy. *Epilepsia* 54, 2048–2059. <http://dx.doi.org/10.1111/epi.1240024117098>.
- 451 Cavazos, J.E., Cross, D.J., 2006. The role of synaptic reorganization in mesial temporal lobe  
452 epilepsy. *Epilepsy & Behavior: E&B* 8 (3), 483–493. <http://dx.doi.org/10.1016/j.yebeh.2006.01.01116500154>.
- 454 Coan, A.C., Campos, B.M., Yasuda, C.L., et al., 2014. Frequent seizures are associated with a  
455 network of gray matter atrophy in temporal lobe epilepsy with or without hippo-  
456 campal sclerosis. *PloS One* 9 (1), e85843. <http://dx.doi.org/10.1371/journal.pone.008584324475055>.
- 457 Cohen, M.S., Kosslyn, S.M., Breiter, H.C., et al., 1996. Changes in cortical activity during  
458 mental rotation. A mapping study using functional MRI. *Brain: A Journal of Neurology*  
459 119 (1), 89–1008624697.
- 461 Friston, K.J., 1994. Functional and effective connectivity in neuroimaging: a synthesis.  
462 *Human Brain Mapping* 2 (1–2), 56–78.
- 463 Glantz, S.A., 2012. *Primer of Biostatistics* seventh edition. McGraw-Hill.
- 464 Guye, M., 2006. The role of corticothalamic coupling in human temporal lobe epilepsy.  
465 *Brain: A Journal of Neurology* 129 (7), 1917–1928. <http://dx.doi.org/10.1093/brain/awl15116760199>.
- Hosmer, D.W., Lemeshow, S., Sturdivant, R.X., 2013. *Applied Logistic Regression* third edi- 467  
468 tion. Wiley, Hoboken, NJ.
- Karunanayaka, P., Kim, K.K., Holland, S.K., Szafarski, J.P., 2011. The effects of left or right 469  
470 hemispheric epilepsy on language networks investigated with semantic decision  
fMRI task and independent component analysis. *Epilepsy & Behavior: E&B* 20, 471  
623–632. <http://dx.doi.org/10.1016/j.yebeh.2010.12.02921273134>.
- Keller, S.S., Gerdes, J.S., Mohammadi, S., et al., 2012. Volume estimation of the thalamus 473  
474 using Freesurfer and stereology: consistency between methods. *Neuroinformatics*  
10 (4), 341–350. <http://dx.doi.org/10.1007/s12021-012-9147-022481382>.
- Keller, S.S., O'Muircheartaigh, J., Traynor, C., Towgood, K., Barker, G.J., Richardson, M.P., 475  
476 2014. Thalamotemporal impairment in temporal lobe epilepsy: a combined MRI  
analysis of structure, integrity, and connectivity. *Epilepsia* 55, 306–315. <http://dx.doi.org/10.1111/epi.1252024447099>.
- Keller, S.S., Roberts, N., 2008. Voxel-based morphometry of temporal lobe epilepsy: an in- 480  
481 troduction and review of the literature. *Epilepsia* 49 (5), 741–757. <http://dx.doi.org/10.1111/j.1528-1167.2007.01485.x18177358>.
- Krauth, A., Blanc, R., Poveda, A., Jeanmonod, D., Morel, A., Székely, G., 2010. A mean three- 483  
484 dimensional atlas of the human thalamus: generation from multiple histological data.  
*NeuroImage* 49 (3), 2053–2062. <http://dx.doi.org/10.1016/j.neuroimage.2009.10.04219853042>.
- Margerison, J.H., Corsellis, J.A., 1966. Epilepsy and the temporal lobes. A clinical, elec- 487  
488 troencephalographic and neuropathological study of the brain in epilepsy, with  
particular reference to the temporal lobes. *Brain: A Journal of Neurology* 89  
489 (3), 499–5305922048.
- Morgan, V.L., Sonmezturk, H.H., Gore, J.C., 2012. Lateralization of temporal lobe epilepsy 491  
492 using resting functional magnetic resonance imaging connectivity of hippocampal  
networks. *Epilepsia* 53 (9), 1628–1635. <http://dx.doi.org/10.1111/j.1528-1167.2012.03590.x22779926>.
- Pardoe, H.R., Pell, G.S., Abbott, D.F., Jackson, G.D., 2009. Hippocampal volume assess- 495  
496 ment in temporal lobe epilepsy: how good is automated segmentation?  
*Epilepsia* 50 (12), 2586–2592. <http://dx.doi.org/10.1111/j.1528-1167.2009.02243.x19682030>.
- Rosenberg, D.S., Mauguière, F., Catenoix, H., Faillenot, I., Magnin, M., 2009. Reciprocal 499  
500 thalamocortical connectivity of the medial pulvinar: a depth stimulation and evoked  
potential study in human brain. *Cerebral Cortex* (New York, N.Y.: 1991) 19 (6),  
1462–1473. <http://dx.doi.org/10.1093/cercor/bhn18518936272>.
- Spencer, S.S., 2002. Neural networks in human epilepsy: evidence of and implications for 503  
504 treatment. *Epilepsia* 43 (3), 219–227. <http://dx.doi.org/10.1046/j.1528-1157.2002.26901.x11906505>.
- Weissenbacher, A., Kasess, C., Gerstl, F., Lanzenberger, R., Moser, E., Windischberger, C. 506  
507 , 2009. Correlations and anticorrelations in resting-state functional connectivity  
MRI: a quantitative comparison of preprocessing strategies. *NeuroImage* 47 (4),  
1408–1416. <http://dx.doi.org/10.1016/j.neuroimage.2009.05.00519442749>.
- Witter, M.P., 1993. Organization of the entorhinal-hippocampal system: a review of cur- 510  
511 rent anatomical data. *Hippocampus* 3 (Spec No 33), 33–448287110.